21. P. V. A. Fine, R. H. Ree, *Am. Nat.* **168**, 796–804 (2006).
22. J. X. Becerra, *Proc. Natl. Acad. Sci. U.S.A.* **102**, 10919–10923 (2005).
23. R. J. Burnham, N. L. Carranco, *Am. J. Bot.* **91**, 1767–1773 (2004).
24. Ministry of the Environment, Peru, *Mapa Nacional de Cobertura Vegetal: Memoria Descriptiva* (Ministerio del Ambiente, Lima, Perú, 2015).
25. L. P. de Queiroz, in *Neotropical Savannas and Seasonally Dry Forests: Plant Diversity, Biogeography, and Conservation*, R. T. Pennington, G. P. Lewis, J. A. Ratter, Eds. (CRC Press, Boca Raton, FL 2006) pp. 121–157.
26. J. Rzedowski, G. C. de Rzedowski, *Acta Bot. Mex.* **102**, 1–23 (2013).
27. R. Linares-Palomino, in *Neotropical Savannas and Seasonally Dry Forest: Plant Diversity, Biogeography and Conservation*, R. T. Pennington, G. P. Lewis, J. A. Ratter, Eds. (CRC Press, Boca Raton, 2006) pp. 227–280.
28. C. E. Hughes, R. T. Pennington, A. Antonelli, *Bot. J. Linn. Soc.* **171**, 1–18 (2013).
29. I. Trejo, R. Dirzo, *Biodivers. Conserv.* **11**, 2063–2084 (2002).
30. S. Bridgewater, J. A. Ratter, J. F. Ribeiro, *Biodivers. Conserv.* **13**, 2295–2317 (2004).
31. D. M. Neves, K. G. Dexter, R. T. Pennington, M. L. Bueno, A. T. Oliveira-Filho, *J. Biogeogr.* **42**, 1566–1576 (2015).
32. K. G. Dexter *et al.*, *Int. For. Rev.* **17**, 10–32 (2015).
33. N. C. A. Pitman *et al.*, *Ecology* **82**, 2101–2117 (2001).
34. H. ter Steege *et al.*, *Science* **342**, 1243092 (2013).
35. G. Forero-Medina, L. Joppa, *PLOS ONE* **5**, e13210 (2010).
36. Convention on Biological Diversity, Quick guide to the Aichi Biodiversity Targets: Protected areas increased and improved, TARGET 11—Technical Rationale extended (COP/10/INF/12/Rev, Convention on Biological Diversity, 2011); https://www.cbd.int/doc/strategic-plan/targets/T11-quick-guide-en.pdf.

ACKNOWLEDGMENTS

This paper is the result of the Latin American and Caribbean Seasonally Dry Tropical Forest Floristic Network (DRYFLOR), which has been supported at the Royal Botanic Garden Edinburgh by a Leverhulme Trust International Network Grant (IN-074). This work was also supported by the U.K. Natural Environment Research Council grant NE/I028122/1; Colciencias Ph.D. scholarship 529; Synthesys Programme GBTAF-2824; the NSF (NSF 1118340 and 1118369); the Instituto Humboldt (IAvH)–Red colombiana de investigación y monitoreo en bosque seco; the Inter-American Institute for Global Change Research (IAI; Tropi-Dry, CRN2-021, funded by NSF GEO 0452325); Universidad Nacional de Rosario (UNR); and Consejo Nacional de Investigaciones Científicas y Técnicas (CONICET). The data reported in this paper are available at www.dryflor.info. R.T.P. conceived the study. M.P., A.O.-F., K.B.-R., R.T.P., and J.W. designed the DRYFLOR database system. K.B.-R. and K.G.D. carried out most analyses. K.B.-R. R.T.P., and K.G.D. wrote the manuscript with substantial input from A.D.-S., R.L.-P., A.O.-F., D.P., C.Q., and R.R. All the authors contributed data, discussed further analyses, and commented on various versions of the manuscript. K.B.-R. thanks G. Galeano who introduced her to dry forest research. We thank J. L. Marcelo, I. Huamantupa, C. Reynel, S. Palacios, and A. Daza for help with fieldwork and data entry in Peru.

DRYFLOR authors

Karina Banda-R,[1,9] Alfonso Delgado-Salinas,[2] Kyle G. Dexter,[1,3] Reynaldo Linares-Palomino,[4,10] Ary Oliveira-Filho,[5] Darién Prado,[6] Martin Pullan,[1] Catalina Quintana,[7] Ricarda Riina,[8] Gina M. Rodríguez M.,[9] Julia Weintritt,[1] Pedro Acevedo-Rodríguez,[11] Juan Adarve,[12] Esteban Álvarez,[13] Anairamiz Aranguren B.,[14] Julián Camilo Arteaga,[15] Gerardo Aymard,[16] Alejandro Castaño,[17] Natalia Ceballos-Mago,[18] Álvaro Cogollo,[13] Hermes Cuadros,[19] Freddy Delgado,[20] Wilson Devia,[21] Hilda Dueñas,[15] Laurie Fajardo,[22] Ángel Fernández,[23] Miller Ángel Fernández,[24] Janet Franklin,[25] Ethan H.Freid,[26] Luciano A. Galetti,[6] Reina Gonto,[23] Roy González-M.,[27,44] Roger Graveson,[28] Eileen H. Helmer,[29] Álvaro Idárraga,[30] René López,[31] Humfredo Marcano-Vega,[29] Olga G. Martínez,[32] Hernán M. Maturo,[6] Morag McDonald,[33] Kurt McLaren,[34] Omar Melo,[35] Francisco Mijares,[36] Virginia Mogni,[6] Diego Molina,[30] Natalia del Pilar Moreno,[37] Jafet M. Nassar,[22] Danilo M. Neves,[1,45] Luis J. Oakley,[6] Michael Oatham,[38] Alma Rosa Olvera-Luna,[2] Flávia F. Pezzini,[1] Orlando Joel Reyes Dominguez,[39] María Elvira Ríos,[40] Orlando Rivera,[37] Nelly Rodríguez,[41] Alicia Rojas,[42] Tiina Särkinen,[1] Roberto Sánchez,[40] Melvin Smith,[28] Carlos Vargas,[43,44] Boris Villanueva,[35] R. Toby Pennington[1]

[1]Royal Botanic Garden Edinburgh, 20a Inverleith Row, EH3 5LR, Edinburgh, UK. [2]Departamento de Botánica, Universidad Nacional Autónoma de México, México D.F., México. [3]School of GeoSciences, University of Edinburgh, Edinburgh, UK. [4]Universidad Nacional Agraria La Molina, Avenida La Molina, Lima, Perú. [5]Universidade Federal de Minas Gerais (UFMG), Instituto de Ciências Biológicas (ICB), Departamento de Botânica, Avenida Antônio. Carlos, 6627-Pampulha, Belo Horizonte, Minas Gerais, Brazil. [6]Cátedra de Botánica, IICAR-CONICET, Facultad de Ciencias Agrarias, Universidad Nacional de Rosario, C.C. Nº 14, S2125ZAA Zavalla, Argentina. [7]Pontificia Universidad Católica del Ecuador, Facultad de Ciencias Exactas, Escuela de Biología, Avenida 12 de Octubre 1076 y Roca, Quito, Ecuador. [8]Real Jardín Botánico, RJB-CSIC, Plaza de Murillo 2, 28014 Madrid, Spain. [9]Fundación Ecosistemas Secos de Colombia, Calle 5 A No. 70 C-31, Bogotá, Colombia. [10]Smithsonian Conservation Biology Institute, Los Libertadores 215, San Isidro, Lima, Perú. [11]Smithsonian National Museum of Natural History, West Loading Dock, 10th and Constitution Avenue, NW, Washington, DC 20560-0166, USA. [12]Parque Regional "El Vínculo"–INCIVA, El Vínculo–Kilometro 3 al sur de Buga sobre la Carretera Panamericana, Valle del Cauca, Colombia. [13]Jardín Botánico de Medellín "Joaquín Antonio Uribe," Calle 73 No. 51D-14, Medellín, Colombia. [14]Instituto de Ciencias Ambientales y Ecológicas, Facultad de Ciencias, Núcleo Pedro Rincón, La Hechicera, 3er Piso, Universidad de los Andes (ULA), Mérida, Venezuela. [15]Herbario SURCO, Universidad Surcolombiana, Neiva, Colombia. [16]Programa de Ciencias del Agro y el Mar, Herbario Universitario (PORT), UNELLEZ-Guanare, Mesa de Cavacas, Estado Portuguesa 3350, Venezuela. [17]Jardín Botánico "Juan María Céspedes" INCIVA, Mateguadua, Tuluá, Valle del Cauca, Colombia. [18]Proyecto Mono de Margarita and Fundación Vuelta Larga, Isla de Margarita, Estado Nueva Esparta, Venezuela. [19]Universidad del Atlántico, Kilometro 7 Vía Puerto, Barranquilla, Atlántico, Colombia. [20]Centro de Investigaciones y Servicios Ambientales (ECOVIDA), Delegación Territorial del Ministerio de Ciencia, Tecnología, y Medio Ambiente, Pinar del Río, Cuba. [21]Unidad Central del Valle del Cauca (UCEVA), Carrera 25 B No. 44-28, Tulúa, Valle del Cauca, Colombia. [22]Centro de Ecología, Instituto Venezolano de Investigaciones Científicas, Apartado 20632, Caracas 1020-A, Venezuela. [23]Centro de Biofísica y Bioquímica (Herbarium), Instituto Venezolano de Investigaciones Científicas, Apartado 20632, Caracas 1020-A, Venezuela. [24]Consultant Botanist, Yopal, Casanare, Colombia. [25]School of Geographical Sciences and Urban Planning, Arizona State University, Post Office Box 875302, Tempe, AZ 85287-5302, USA. [26]Bahamas National Trust, Leon Levy Native Plant Preserve, Eleuthera, Bahamas. [27]Instituto de Investigación de Recursos Biológicos Alexander von Humboldt, Avenida Paseo Bolívar 16-20, Bogotá, D.C., Colombia. [28]Consultant Botanist, Cas en Bas Road, Gros Islet, St. Lucia. [29]Forest Service, Southern Research Station, International Institute of Tropical Forestry, Jardín Botánico Sur, 1201 Calle Ceiba, San Juan, PR00926, Puerto Rico. [30]Grupo de Estudios Botánicos, Universidad de Antioquia, AA 1226 Medellín, Colombia. [31]Universidad Distrital Francisco José de Caldas, Carrera 5 Este No. 15-82, Bogotá, Colombia. [32]Facultad de Ciencias Naturales, Universidad Nacional de Salta, Avenida Bolivia 5150, 4400 Salta, Argentina. [33]School of Environment, Natural Resources, and Geography, Thoday Building, Room G21, Bangor University, Bangor LL57 2DG, UK. [34]Department of Life Sciences, University of West Indies, Mona, Jamaica. [35]Universidad del Tolima, Barrio Santa Helena Parte Alta, Código Postal 730006299, Ibagué, Tolima, Colombia. [36]Fundación Orinoquia Biodiversa, Calle 15 No. 12-15, Tame, Arauca, Colombia. [37]Instituto de Ciencias Naturales, Universidad Nacional de Colombia, Sede Bogotá, Código Postal 111321, Avenida Carrera 30 No. 45-03, Edificio 425, Bogotá, Colombia. [38]Department of Life Sciences, The University of The West Indies St. Augustine, Natural Sciences Building, Old Wing, Room 222, St. Augustine, Trinidad and Tobago. [39]Centro Oriental de Ecosistemas y Biodiversidad BIOECO, Cuba. [40]Universidad de Pamplona, Ciudad Universitaria, Pamplona, Norte de Santander, Colombia. [41]Departamento de Biología, Universidad Nacional de Colombia, Sede Bogotá, Código Postal 111321, Avenida Carrera 30 No. 45-03, Edificio 476, Bogotá, Colombia. [42]Jardín Botánico Eloy Valenzuela, Avenida Bucarica, Floridablanca, Santander, Colombia. [43]Jardín Botánico de Bogotá "José Celestino Mutis," Avenida Calle 63 No. 68-95, Bogotá, Colombia. [44]Facultad de Ciencias Naturales y Matemática, Universidad del Rosario, Carrera 26 No. 63B-48, Bogotá, Colombia. [45]Royal Botanic Gardens, Kew, Richmond, Surrey, UK.

SUPPLEMENTARY MATERIALS

www.sciencemag.org/content/353/6306/1383/suppl/DC1
Materials and Methods
Figs. S1 to S6
Tables S1 to S6
References (*37*–*45*)

26 February 2016; accepted 11 August 2016
10.1126/science.aaf5080

INFECTIOUS DISEASE

Replication of human noroviruses in stem cell–derived human enteroids

Khalil Ettayebi,[1]* Sue E. Crawford,[1]* Kosuke Murakami,[1]* James R. Broughman,[1] Umesh Karandikar,[1] Victoria R. Tenge,[1] Frederick H. Neill,[1] Sarah E. Blutt,[1] Xi-Lei Zeng,[1] Lin Qu,[1] Baijun Kou,[1] Antone R. Opekun,[2,3,4] Douglas Burrin,[3,4] David Y. Graham,[1,2,5] Sasirekha Ramani,[1] Robert L. Atmar,[1,2] Mary K. Estes[1,2]†

The major barrier to research and development of effective interventions for human noroviruses (HuNoVs) has been the lack of a robust and reproducible in vitro cultivation system. HuNoVs are the leading cause of gastroenteritis worldwide. We report the successful cultivation of multiple HuNoV strains in enterocytes in stem cell–derived, nontransformed human intestinal enteroid monolayer cultures. Bile, a critical factor of the intestinal milieu, is required for strain-dependent HuNoV replication. Lack of appropriate histoblood group antigen expression in intestinal cells restricts virus replication, and infectivity is abrogated by inactivation (e.g., irradiation, heating) and serum neutralization. This culture system recapitulates the human intestinal epithelium, permits human host-pathogen studies of previously noncultivatable pathogens, and allows the assessment of methods to prevent and treat HuNoV infections.

Human noroviruses (HuNoVs) are the most common cause of epidemic and sporadic cases of acute gastroenteritis worldwide, and are the leading cause of food-borne gastroenteritis (*1*–*3*). Since the introduction of rotavirus vaccines, HuNoVs have become the predominant gastrointestinal pathogen within pediatric populations in developed countries (*4*). HuNoVs are highly contagious, with rapid person-to-person transmission directly through the fecal-oral route

and indirectly from contact with contaminated fomites or by consumption of contaminated food or water. In addition to causing morbidity and mortality in young children, immunocompromised patients, and the elderly, norovirus disease causes substantial economic burden as a result of health care costs and loss of productivity (*5*, *6*). HuNoVs have resisted efforts to establish in vitro cultivation methods for more than 40 years. Previous reports of possible cultivation systems have not been reproduced or support limited replication of a single strain (*7*–*10*). Insight into the pathophysiology of HuNoV infections has been elucidated primarily from studies using healthy adult volunteers. The lack of a reproducible culture system for HuNoVs has remained the major barrier to achieving a full mechanistic understanding of their replication, stability, antigenic complexity, and evolution. An in vitro cultivation system is critical to define HuNoV-host interactions that underlie the high virus infectivity and explosive illness they cause, to determine how to prevent transmission, and to treat infections and illness.

[1]Department of Molecular Virology and Microbiology, Baylor College of Medicine, Houston, TX, USA. [2]Department of Medicine, Baylor College of Medicine, Houston, TX, USA. [3]Section of Gastroenterology, Hepatology and Nutrition, Department of Pediatrics, Baylor College of Medicine, Houston, TX, USA. [4]USDA/ARS Children's Nutrition Research Center, Houston, TX, USA. [5]Department of Medicine, Michael E. DeBakey VA Medical Center, Houston, TX, USA.
*These authors contributed equally to this work. †Corresponding author. Email: mestes@bcm.edu

Ex vivo human intestinal enteroid cultures support HuNoV replication

Attempts to culture HuNoVs in transformed intestinal epithelial cells and in primary human immune cells have been unsuccessful (*8*, *11*, *12*). We hypothesized that a novel culture system pioneered by the Clevers group in the Netherlands, which generates human intestinal enteroids (HIEs) from stem cells isolated from intestinal crypts in human intestinal tissues (*13*, *14*) and recapitulates the natural intestinal epithelium, should support HuNoV growth. These multicellular, differentiated HIEs are nontransformed, physiologically active cultures that respond to agonists and contain multiple intestinal epithelial cell types (enterocytes, goblet, enteroendocrine, and Paneth cells), whether grown as three-dimensional or monolayer cultures (fig. S1) (*13*–*16*).

To evaluate whether these novel cultures support replication of the previously noncultivatable HuNoVs, we inoculated monolayers of HIEs with GII.4 HuNoVs, which cause the majority of pandemic and outbreak infections worldwide (*1*). Jejunal monolayer cultures were readily infected by stool filtrates of multiple GII.4 variants (GII.4/2006a, GII.4/2006b-1 to -3, GII.4/2009, and GII.4/2012-1 and -2; table S1). At 96 hours post-infection

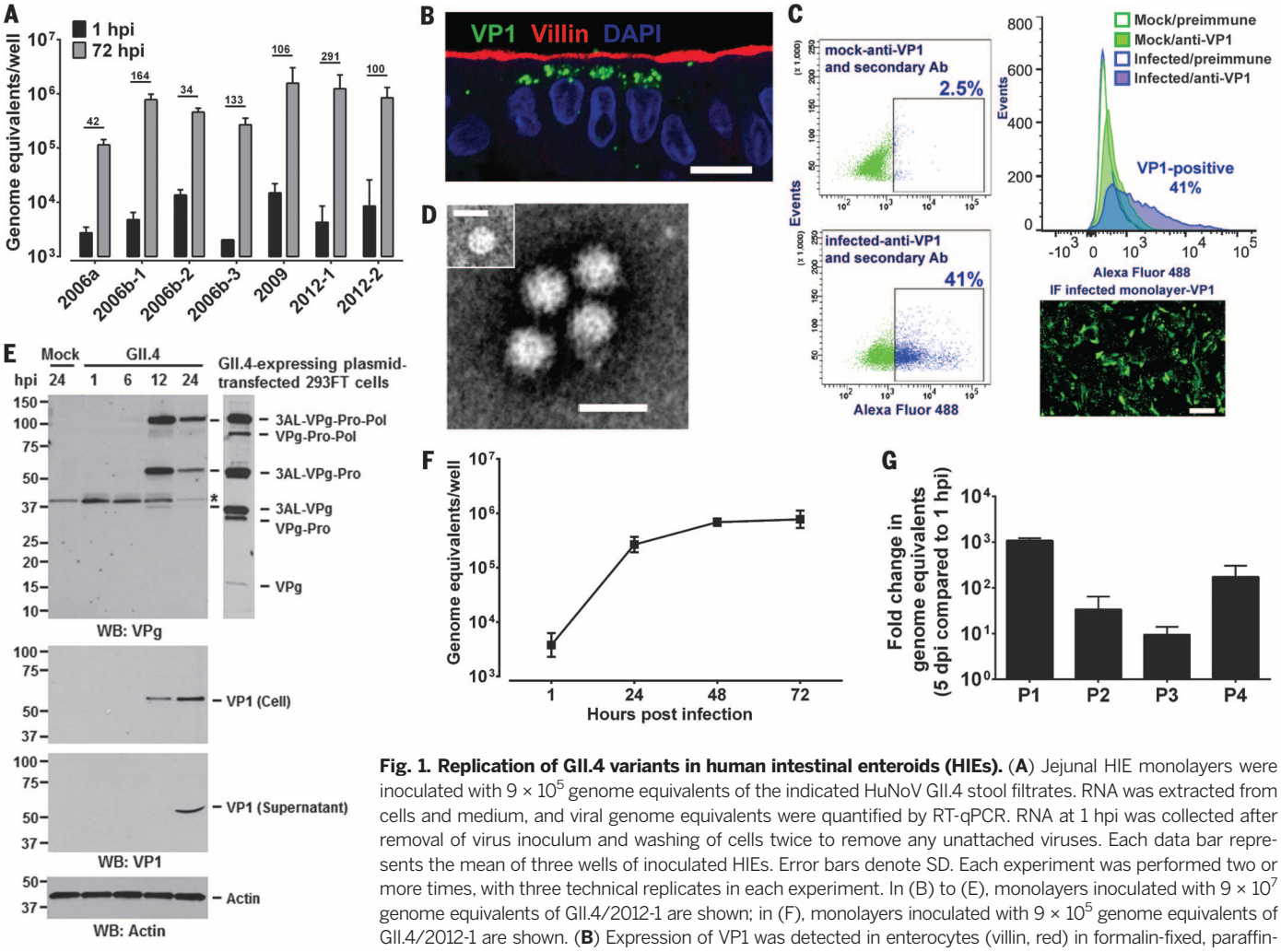

Fig. 1. Replication of GII.4 variants in human intestinal enteroids (HIEs). (**A**) Jejunal HIE monolayers were inoculated with 9×10^5 genome equivalents of the indicated HuNoV GII.4 stool filtrates. RNA was extracted from cells and medium, and viral genome equivalents were quantified by RT-qPCR. RNA at 1 hpi was collected after removal of virus inoculum and washing of cells twice to remove any unattached viruses. Each data bar represents the mean of three wells of inoculated HIEs. Error bars denote SD. Each experiment was performed two or more times, with three technical replicates in each experiment. In (B) to (E), monolayers inoculated with 9×10^7 genome equivalents of GII.4/2012-1 are shown; in (F), monolayers inoculated with 9×10^5 genome equivalents of GII.4/2012-1 are shown. (**B**) Expression of VP1 was detected in enterocytes (villin, red) in formalin-fixed, paraffin-embedded enteroid monolayer sections using antibody against GII.4/2012 VLPs (green). DAPI (4′,6-diamidino-2-phenylindole) detects nuclei (blue). Scale bar, 25 μm. (**C**) Flow cytometry quantitation and immunofluorescent detection of infected cells. Scale bar, 100 μm. (**D**) Electron micrograph of HuNoV particles from the supernatant of infected HIEs. Scale bar, 50 nm. Inset: small particle. Scale bar, 25 nm. (**E**) Western blot detecting polyprotein processing and VP1 expression. Asterisk marks a nonspecific band. (**F**) Kinetics of HuNoV yield at the indicated time points. (**G**) Passaging of GII.4/2009 HuNoV in jejunal HIEs. In (F) and (G), viral genome equivalents were quantified by RT-qPCR as in (A).

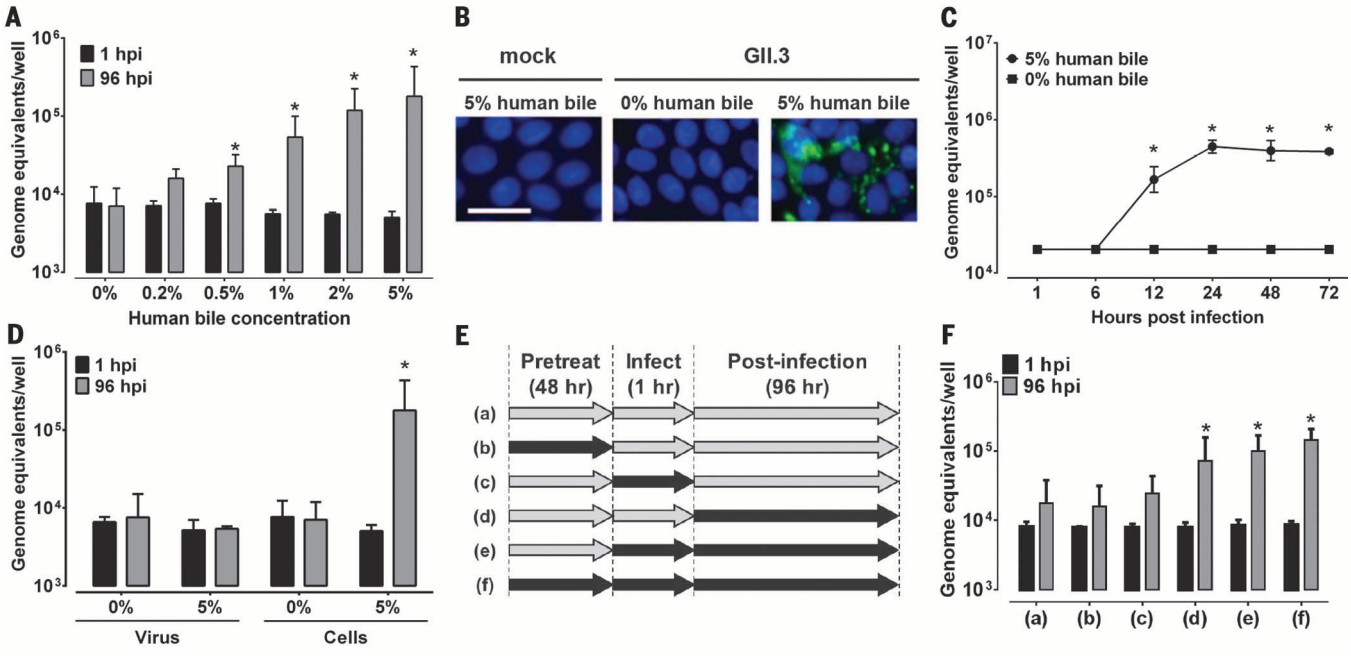

Fig. 2. Bile is required for GII.3 HuNoV replication and affects the cells. (**A** to **C**) Jejunal HIE monolayers were pretreated with the indicated concentrations of human bile for 2 days and then inoculated with GII.3 stool filtrate [(A) and (C), 4.3×10^5 genome equivalents; (B), 4.3×10^7 genome equivalents] and incubated with the same bile concentrations as used for pretreatment (see supplementary materials). (B) VP1 was detected in methanol-fixed monolayers at 24 hpi using guinea pig anti-GII.3 VLP antiserum (green) and DAPI to detect nuclei (blue). Scale bar, 25 μm. (**D**) Determination of effect of bile treatment on virus or cells. Virus was either not treated or treated with 5% human bile for 1 hour at 37°C, and then diluted to decrease the bile concentration to 0.025% before infection of HIE monolayers not pretreated with bile; cells were either not treated or treated with 5% human bile for 2 days before and during infection. Inoculations were performed with 4.3×10^5 genome equivalents. (**E**) Schematic showing with black arrows when bile was added to HIEs for the experiment shown in (F). (**F**) HIE monolayers treated with bile as indicated in (E) were infected with 4.3×10^5 genome equivalents of GII.3 stool filtrate. For (A), (C), (D), and (F), genome equivalents were determined as indicated in Fig. 1. Error bars denote SD. *$P < 0.05$ comparing genome equivalents to 1 hpi.

(hpi), 1.5 to 2.5 $\log_{10}$ increases in genome equivalents of viral progeny were identified by reverse transcription–quantitative polymerase chain reaction (RT-qPCR) in comparison to the amount of genomic RNA detected at 1 hpi after removal of the virus inoculum and two washes of the monolayers to remove unattached virus (Fig. 1A, relative changes indicated above the bars for each variant). All inocula used to infect enteroid cultures were fecal filtrates, which suggests that bacteria were not required as cofactors for infection, in contrast to previous reports of HuNoV cultivation in BJAB and Raji B cell lines (*9*, *10*). Lipopolysaccharide (LPS) in stool filtrates did not promote replication, as there was no reduction in HuNoV replication in samples treated with polymyxin B that reduced LPS levels from 4.84 to 0.63 endotoxin units (*12*) (fig. S2A).

We next evaluated the growth characteristics of HuNoV infection by assessing cytopathic effect (CPE), antigen detection, and the kinetics of infection. Cytopathic changes such as cell rounding, destruction of the monolayer, and an increase in the number of dead cells as assessed by trypan blue staining were observed in GII.4-inoculated cultures. CPE was observed for the tested GII.4 variants GII.4/2012-1, GII.4/2012-2, and GII.4/2006b-3 (see table S1 for strain details; GII.4/2012-1 results shown in fig. S2B, left panel). CPE was not reduced by inoculation with polymyxin B–treated samples (fig. S2B), and CPE was not observed in cultures inoculated with γ-irradiated stool filtrate (fig. S2B, right panels), which abrogated viral replication. Viral replication was demonstrated by detecting the major viral capsid protein (VP1) with nonstructural proteins [RNA-dependent RNA polymerase (Pol) and nucleotide triphosphatase (NTPase)] or double-stranded RNA (dsRNA, an intermediate in HuNoV RNA replication) in infected cells by confocal microscopy (Fig. 1B and fig. S3, A to C). Immunofluorescent analysis for VP1 revealed that 35 to 45% of cells in the HIE monolayer were infected, which was confirmed by flow cytometry where 41% of cells were VP1-positive (Fig. 1C). HIE cultures contain multiple cell types (stem cells, Paneth cells, and goblet, enteroendocrine, and enterocyte cells), and only the enterocytes were infected. Detection of villin, an enterocyte marker, in VP1-positive cells showed that HuNoVs infected and replicated in enterocytes (Fig. 1B).

Productive infection was confirmed by transmission electron microscopy, which yielded images of virus particles with typical morphology (*17*) in the supernatant of infected HIEs (Fig. 1D). Two particle sizes were detected (Fig. 1D), with particles of the expected size (31.6 ± 3.3 nm) and some smaller particles (18.5 ± 3.7 nm; Fig. 1D, inset). Both particle sizes have been observed previously in stools of children infected with HuNoVs and in preparations of recombinant virus-like particles (VLPs) (*18*). By Western blot analysis, nonstructural polyprotein synthesis and processing [as evidenced by the detection of several viral protein genome-linked (VPg)–containing polyprotein processing intermediates] and capsid protein (VP1) production were first detected at 12 hpi in infected cells but not at 1 or 6 hpi or in mock-infected cells (Fig. 1E). Consistent with the production of virus particles (Fig. 1D), VP1 was detected in the culture supernatant by 24 hpi (Fig. 1E). Replication was confirmed by the growth kinetics of GII.4/2012-1 in jejunal HIE monolayer cultures, which showed a time-dependent increase in genome equivalents between 1 and 24 hpi, after which a plateau was reached (Fig. 1F). Because polyprotein processing, RNA replication, and synthesis of subgenomic RNA are required for VP1 and particle production (*19*), these findings demonstrate that an entire HuNoV replication cycle occurs in infected HIEs by 24 hpi. GII.4/2009 and GII.4/2012-1 HuNoV could also be passaged in jejunal HIEs with optimized conditions (Fig. 1G, GII.4/2009 shown; see below for conditions). Cells expressing VP1 and VPg were observed during infection with passaged virus (fig. S4A), and particles of both sizes (fig. S4B) were seen. Together, these results indicate that GII.4 HuNoV infection of HIEs results in a productive and complete virus replication cycle,

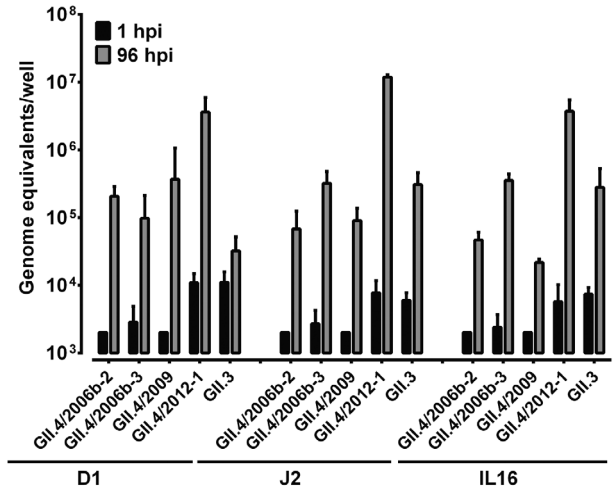

Fig. 3. GII.4 variants and GII.3 HuNoVs replicate in HIEs generated from different intestinal segments. Duodenal (D1), jejunal (J2), and ileal (IL16) HIEs were treated with 1% sow bile for the GII.4 variants or 5% human bile for GII.3 for 48 hours, and then inoculated with the indicated HuNoVs (GII.4/2006b-2, GII.4/2009, and GII.4/2012-1, 9×10^5 genome equivalents; GII.4/2006b-3, 5.5×10^5 genome equivalents; GII.3, 4.3×10^5 genome equivalents) and cultured in the presence of bile. Genome equivalents were determined as indicated in Fig. 1. Error bars denote SD.

and that this system can be used to define cellular processes that HuNoVs co-opt to replicate and induce pathogenesis.

Replication of some HuNoV strains requires the presence of bile

Noroviruses are genetically diverse. Most HuNoVs are classified into two genogroups (GI and GII), which are further subdivided into nine GI genotypes and 20 GII genotypes. We next tested whether monolayer cultures of jejunal HIEs could support replication of other HuNoV strains (GI.1, GII.3, GII.17). Initially, no replication of these viruses was observed. Consequently, several components of the intestinal milieu were assessed for their ability to promote replication of these HuNoVs in HIE monolayers. Addition of proteases (trypsin, pancreatin) required for the replication of another gastrointestinal virus, human rotavirus, failed to enhance HuNoV replication. In contrast, viral replication, as demonstrated by RT-qPCR and immunofluorescence analyses, was observed in HIEs pretreated with nontoxic levels of human bile and inoculated with stool filtrates of GII.3, GII.17, and GI.1 HuNoVs (Fig. 2, A and B, and fig. S5). Replication occurred in a bile dose–dependent manner, with concentrations of human bile greater than or equal to 0.5% being required for GII.3 replication (Fig. 2A). Bile from different sources, such as human, sow, and commercially available bovine and porcine, all promoted GII.3 replication without CPE (fig. S6). Assessment of the kinetics of GII.3 infection demonstrated that, similar to GII.4 strains, virus yields increased between 1 and 24 hpi (Fig. 2C). The addition of bile to GII.4 HuNoV-inoculated cultures was not required, but it enhanced virus replication (fig. S7). Enhancement was observed when human (fig. S7A), piglet (fig. S7B), porcine (fig. S7C), and sow (fig. S7D) bile were evaluated.

These results indicate that there are strain-specific differences in the requirement for factors in the intestinal milieu such as bile to support or enhance HuNoV replication. Of note, even with the addition of bile, the increases in yields for GII.3 as well as for GII.17 and GI.1 virus strains were lower than that observed for the GII.4 variants. In 12 independent experiments performed in triplicate on jejunal HIEs, the mean relative increase of GII.3 genome equivalents from 1 hpi to a later time point ranged from a factor of 10 to a factor of 173 (average increase, factor of 48); for GII.4 HuNoVs, the mean relative increase ranged from a factor of 34 to a factor of 6730 (average increase, factor of 670). Evaluation of additional intestinal components or further optimization of conditions may be required to achieve higher levels of replication for GII.3 and other HuNoVs. To date, we have successfully obtained replication of two HuNoV genogroups comprising four genotypes of virus (including four GII.4 variants and GII.3, GII.17, and GI.1 strains) in human jejunal enteroid monolayers (table S1).

We next evaluated whether the requirement of bile for GII.3 HuNoV infection and replication was due to a bile effect on the HIE cells or on the virus. Stool filtrate was pretreated with 5% bile or phosphate-buffered saline (PBS) for 1 hour and then diluted in PBS (final concentration of 0.025% in the bile-treated sample) prior to inoculating HIE cultures not treated with bile. HIEs also were either not treated or treated with 5% bile for 48 hours prior to and during infection. The pretreatment of cells with bile was carried out for a longer duration as compared to pretreatment of the virus with bile because bile has multiple known effects on cellular functions, including acting as a detergent, increasing digestion and absorption of fat, and regulating metabolic and inflammatory processes by activating various signaling pathways (*20*). An increase in genome equivalents was observed only when HIE cells were treated with bile (Fig. 2D), indicating that the bile effect is on the cells and not on the virus.

Further assessment of bile treatment revealed that addition of bile to cultures during or after virus adsorption, but not prior to adsorption, is required for GII.3 replication (Fig. 2, E and F). Testing of heat- or trypsin-treated bile for GII.3 infections in HIEs found no effect on replication (fig. S8), indicating that the active factor is not proteinaceous. The successful cultivation of GII.3 HuNoV required both novel HIE cultures and supplementary bile, because the addition of bile to transformed epithelial cell lines including Huh7, Vero, HEK293FT, and undifferentiated or differentiated Caco-2 BBe cells did not promote HuNoV replication (fig. S9). These results indicate that HIEs and bile together mimic the human replication niche of HuNoVs.

The sensitivity of the HIE culture system to support HuNoV replication was evaluated by determining the lower limit of virus required for successful infection. For this, the dose required to produce infection in 50% of the inoculated cultures (ID_{50}) for GII.4 and GII.3 HuNoVs was calculated by the Reed-Muench method (*21*). The ID_{50} values for GII.4/2012-1 and GII.3 HuNoVs were ~1200 and ~2.0×10^4 genome equivalents per well, respectively, assessed at 7 days post-infection (dpi; geometric mean of two experiments, representative experiments shown in fig. S10, A and B). These results indicate that this replication system is amenable to determining the infectivity of low levels of virus, as has been observed in emesis, contaminated food, and fecal samples after recovery from illness (*8*, *22*, *23*). This replication system also will allow evaluation of whether a given virus, currently detected in a variety of samples by molecular methods, is infectious and poses a potential risk to human health.

HuNoVs replicate in enterocytes in cultures from different segments of the small intestine

The site of replication of HuNoVs in immunocompetent individuals is unknown, although histologic alterations have been observed in small

Table 1. Comparison of BT50 and 50% neutralization titers. BT50 denotes a serum titer that blocks the interaction of HuNoV VLPs with H type 1 and H type 3 and porcine gastric mucin glycans by 50%; 50% neutralization denotes a serum titer that reduces the infectivity of indicated HuNoV strains by 50%.

Serum	GII.3		GII.4	
	BT50	50% neutralization	BT50	50% neutralization
1	187	990	671	105,000
2	70	835	53	214

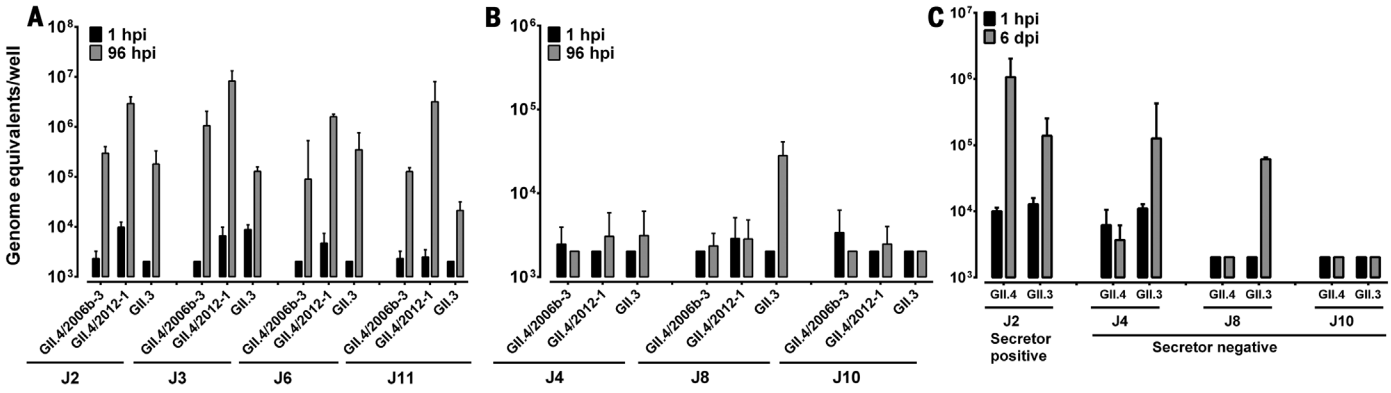

Fig. 4. Replication of GII.4 strains but not GII.3 depends on HIE secretor status. (**A**) Secretor-positive jejunal (J2, J3, J6, and J11) or (**B**) secretor-negative jejunal (J4, J8, and J10) HIEs were inoculated with the indicated GII.4 or GII.3 HuNoVs (with the same amounts of genome equivalents as indicated in Fig. 3) in the presence of bile (1% sow bile for GII.4 variants or 5% human bile for GII.3) for 96 hours. At 96 hpi, GII.4 strains replicate in secretor-positive HIEs but not secretor-negative lines, while GII.3 replicates in all secretor HIEs and one secretor-negative line (J8). (**C**) At 6 dpi, the GII.3 virus shows replication in an additional secretor-negative HIE (J4) while no growth of GII.4/2012-1 virus is seen. A secretor J2 HIE is included as control to show replication of GII.4 at 6 dpi. In (A) to (C), genome equivalents were determined as indicated in Fig. 1. Error bars denote SD.

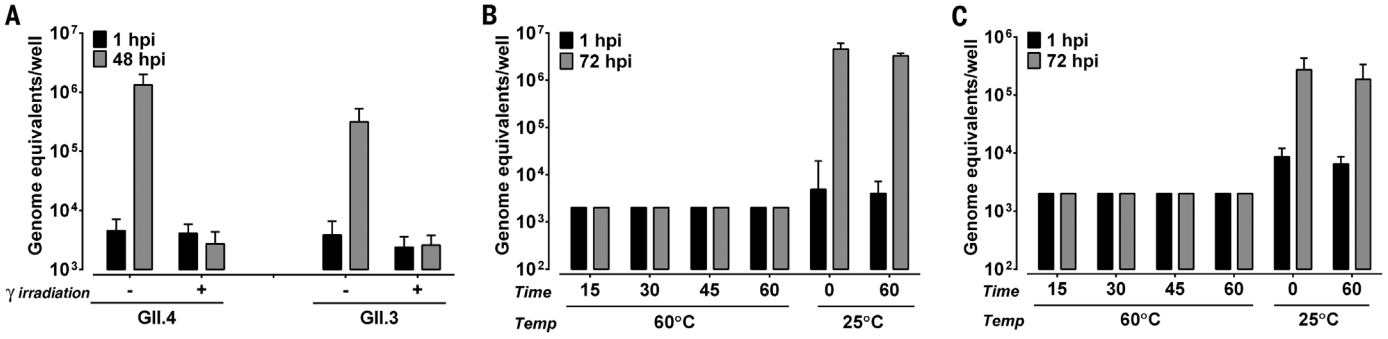

Fig. 5. Inactivation of GII.4 and GII.3 HuNoV infectivity by γ irradiation and heat treatment. (**A**) GII.4/2012-1 and GII.3 HuNoVs were γ-irradiated or incubated at room temperature overnight. (**B** and **C**) GII.4/2012-1 (9×10^5 genome equivalents) (B) or GII.3 (4.3×10^5 genome equivalents) (C) were heat-inactivated at 60°C for the indicated time points or incubated at room temperature for 0 and 60 min. Jejunal HIEs were inoculated with each sample. Genome equivalents were determined as shown in Fig. 1. Error bars denote SD.

intestinal biopsies from volunteers infected with Norwalk virus (*24*) and antigen has been detected in duodenal, jejunal, and (to a lesser extent) ileal enterocytes from gnotobiotic pigs infected with a GII.4 HuNoV (*25*). We therefore evaluated whether HuNoVs infect cells derived from different regions of the small intestine by inoculating HIE cultures made from biopsies obtained from different intestinal segments that retain segment-specific properties (*26*). GII.4 and GII.3 HuNoVs replicated in enteroids derived from duodenal, jejunal, and ileal intestinal segments (Fig. 3). Replication varied by strain and intestinal segment, with GII.4 variants showing increases by factors of 11 to 1535 between 1 and 96 hpi in the three segments and GII.3 virus showing increases by factors of 3 to 51.

We investigated whether HuNoVs replicated in cell types other than enterocytes. HuNoV antigen was not detected in goblet cells (n = 200) or enteroendocrine cells (n = 50) assessed in duodenal, jejunal, and ileal HIEs. Together, the growth of HuNoVs in HIEs from all segments of the small intestine detected by RNA replication and confocal staining indicates that enterocytes (Fig. 1B) are the primary target for infection and replication.

Secretor status of HIEs affects strain-specific HuNoV replication

HuNoV infection is dependent on expression of genetically determined histoblood group antigens (HBGAs), and genetic resistance to some HuNoV genotypes has been documented in challenge and outbreak studies (*27*). The presence of a functional fucosyltransferase 2 (FUT2, secretor-positive genotype) enzyme, which transfers fucose to HBGA precursors in gastrointestinal cells in secretor-positive persons, correlates with susceptibility to infection with most GII.4 HuNoVs. We generated HIEs from secretor-positive and -negative persons to determine whether these cultures recapitulate genotype-specific patterns of HuNoV susceptibility (*14*). All secretor-positive jejunal HIEs supported productive replication of GII.4 variants (by factors of 44 to 1270) and GII.3 HuNoVs (by factors of 10 to 173), as assessed by increases in genome equivalents between 1 and 96 hpi (Fig. 4A). In contrast, GII.4 strains did not infect HIEs generated from secretor-negative individuals when assayed at 96 hpi or 6 dpi (Fig. 4, B and C, respectively). However, GII.3 virus infected two of three secretor-negative HIEs, one of which was positive only after 6 days in culture (Fig. 4, B and C, respectively). These results mirror epidemiologic data showing that GII.3 HuNoVs, but not GII.4 HuNoVs, can infect some individuals (*27*) and indicate that HuNoV infection of HIEs is a biologically relevant system that mimics infections in genetically defined individuals. Further analysis of genetically defined HIEs will aid in determining additional host susceptibility factors to infection.

HuNoV cultivation in HIEs allows evaluation of virus neutralization and inactivation

Functional antibodies in serum that block the binding of HuNoV VLPs to HBGAs correlate with protection against clinical gastroenteritis in volunteer challenge and vaccination studies (*28*–*30*). HBGA-blocking assays examine the ability of human serum to block the interaction

of HuNoV VLPs with H type 1 and H type 3 glycans and porcine gastric mucin (*31*, *32*), and the antibody titer that results in 50% blocking (BT50) has been used as a surrogate for virus neutralization (*28*). We used the HIE cultivation system to directly measure virus neutralization. Neutralizing antibody titers (the reciprocal antibody dilution present in serum able to reduce virus yields by 50% relative to virus incubated in media alone) were compared to HBGA-blocking titers. Serum samples from two individuals, one with a high BT50 and another with a low BT50 against GII.4 VLPs, were tested (Table 1). Both samples had low BT50s against GII.3 VLPs. The neutralization titers were higher than the BT50 values (Table 1 and fig. S11, A to D) and virus-induced CPE was neutralized (fig. S11E); these findings suggest that virus neutralization is a more sensitive assay than the HBGA blocking assay, and that neutralization epitopes other than HBGA-blocking epitopes may exist on norovirus particles.

The previous inability to cultivate HuNoVs has hampered the development of strategies to control and prevent HuNoV infection, and has limited the ability to determine the effectiveness of existing methods to inactivate virus to prevent transmission in various settings, including in food or on contaminated surfaces. The persistence of HuNoVs in the environment, their high transmissibility, and the problem of chronic infection of immunocompromised individuals document a need for antiviral treatment and prophylaxis of norovirus infections. To determine whether the HIE infection model is suitable for testing virus inactivation, we evaluated GII.3 and GII.4 HuNoV inactivation by γ irradiation and heat treatment. No growth was observed after γ irradiation of either GII.4 or GII.3 HuNoVs (Fig. 5A). Compared to incubation of GII.4 or GII.3 viruses at room temperature for 60 min, heating at 60°C for as little as 15 min inactivated both viruses; no increase in yield was detected from 1 to 72 hpi (Fig. 5, B and C). These studies indicate that HuNoV infection of HIEs will allow evaluation of new methods to inactivate HuNoVs and to measure the effectiveness of disinfectants and sanitizers, including characterization of the efficacy of both traditional and novel control measures.

Implications of in vitro replication of HuNoV for understanding its biology

HuNoV was visualized by Albert Kapikian in 1972 (*17*), but conditions to grow these viruses in vitro have remained an unsolved mystery for more than 40 years. Our results show that HuNoV replication in HIEs is robust, based on achieving several $\log_{10}$ increases in replication of multiple variants of the epidemiologically predominant GII.4 HuNoVs in HIE lines from different small intestinal segments from multiple immunocompetent individuals; replication was documented by expression of structural and nonstructural proteins, production and release of virus particles into culture supernatants, and successful passaging of virus. The cultivation system described in this study has biologic relevance, with replication of different strains being consistent with known host restriction based on HBGA expression. Variability in replication between different HIE cultures is observed; specific cultures (secretor-positive) are highly susceptible to HuNoV strains, and other cultures (secretor-negative) show variable resistance to infection with specific HuNoV strains. These results mirror infectivity patterns seen in epidemiological studies. Future work with additional strains is needed to understand the basis for this variability, particularly for infection of different secretor-negative lines with GII.3 viruses.

HuNoVs replicate in enterocytes from different intestinal segments in HIEs. In addition, factors present in the intestinal milieu, such as bile, enhance or are required for replication to occur. Bile obtained from various mammalian sources (human, sow, piglet, porcine, and bovine) mediates this effect, although there is variability between bile sources and virus strains. These results are consistent with previous data from intestinal biopsies from HuNoV-infected immunocompromised transplant patients and studies in large animals (gnotobiotic pigs and newborn calves) infected orally with HuNoV GII.4 or bovine norovirus GIII.1 strains, respectively, where enterocytes in different segments of the small intestine are clearly infected and express viral antigen (*25*, *33*, *34*). Filtered stool was used as inoculum in the present study, and bacterial LPS was not required for infectivity. These results differ from reports of cultivation of a single strain of HuNoV in B cells where unfiltered inocula and commensal bacteria are required as cofactors (*9*, *10*), and of HuNoV replication in other animal models following nonoral routes of inoculation, including intraperitoneal injection of immunodeficient mice (*35*) or intravenous injection of chimpanzees (*36*); in those models, virus was not detected in the intestinal epithelium but was detected in cells in the lamina propria, with some expressing DC-SIGN (chimpanzees) or with a macrophage-like morphology (mice).

Replication of HuNoVs in enterocytes in HIEs supports the observation that another site(s) of primary replication besides B cells must exist, because HuNoVs can infect B cell–deficient patients (*37*, *38*). Our results are reminiscent of initial conditions that required the addition of intestinal contents from gnotobiotic piglets to successfully culture a porcine enteric calicivirus (PEC), a member of the *Sapovirus* genus of the Caliciviridae family, using primary porcine kidney cells (*39*). Species-specific bile enhanced primary replication in that system, and subsequent studies showed that bile acids and a continuous porcine kidney cell line can support PEC replication (*40*). Additional studies are needed to determine the active components of bile needed to support HuNoV replication in HIEs. The active component(s) in bile and mechanism(s) of action required for HuNoV cultivation in HIEs remain to be fully characterized, but initial characterization demonstrates that it is not a protein. The establishment of this cultivation system will facilitate applications in many different realms of public health importance—such as food safety and the development of new diagnostics, vaccines, and therapeutics—and will advance research on HuNoV evolution, immunity, and pathogenesis.

REFERENCES AND NOTES

1. S. Ramani, R. L. Atmar, M. K. Estes, *Curr. Opin. Gastroenterol.* **30**, 25–33 (2014).
2. S. M. Ahmed *et al.*, *Lancet Infect. Dis.* **14**, 725–730 (2014).
3. A. J. Hall *et al.*, *Emerg. Infect. Dis.* **19**, 1198–1205 (2013).
4. D. C. Payne *et al.*, *N. Engl. J. Med.* **368**, 1121–1130 (2013).
5. K. Y. Green, *Clin. Microbiol. Infect.* **20**, 717–723 (2014).
6. G. Belliot, B. A. Lopman, K. Ambert-Balay, P. Pothier, *Clin. Microbiol. Infect.* **20**, 724–730 (2014).
7. T. M. Straub *et al.*, *Emerg. Infect. Dis.* **13**, 396–403 (2007).
8. M. D. Moore, R. M. Goulter, L. A. Jaykus, *Annu. Rev. Food Sci. Technol.* **6**, 411–433 (2015).
9. M. K. Jones *et al.*, *Nat. Protoc.* **10**, 1939–1947 (2015).
10. M. K. Jones *et al.*, *Science* **346**, 755–759 (2014).
11. E. Duizer *et al.*, *J. Gen. Virol.* **85**, 79–87 (2004).
12. M. K. Lay *et al.*, *Virology* **406**, 1–11 (2010).
13. T. Sato *et al.*, *Gastroenterology* **141**, 1762–1772 (2011).
14. K. Saxena *et al.*, *J. Virol.* **90**, 43–56 (2016).
15. K. L. VanDussen *et al.*, *Gut* **64**, 911–920 (2015).
16. N. C. Zachos *et al.*, *J. Biol. Chem.* **291**, 3759–3766 (2016).
17. A. Z. Kapikian *et al.*, *J. Virol.* **10**, 1075–1081 (1972).
18. L. J. White, M. E. Hardy, M. K. Estes, *J. Virol.* **71**, 8066–8072 (1997).
19. K. Y. Green, in *Fields Virology*, D. M. Knipe, P. M. Howley, Eds. (Lippincott Williams and Wilkins, 2013), pp. 582–608.
20. A. F. Hofmann, in *Physiology of the Gastrointestinal Tract*, L. R. Johnson, Ed. (Raven, New York, 1994), pp. 1555–1576.
21. L. J. Reed, H. Muench, *Am. J. Hyg.* **27**, 493 (1938).
22. R. L. Atmar *et al.*, *Emerg. Infect. Dis.* **14**, 1553–1557 (2008).
23. F. Le Guyader *et al.*, *Appl. Environ. Microbiol.* **62**, 4268–4272 (1996).
24. S. G. Agus, R. Dolin, R. G. Wyatt, A. J. Tousimis, R. S. Northrup, *Ann. Intern. Med.* **79**, 18–25 (1973).
25. S. Cheetham *et al.*, *J. Virol.* **80**, 10372–10381 (2006).
26. S. Middendorp *et al.*, *Stem Cells* **32**, 1083–1091 (2014).
27. N. Ruvoën-Clouet, G. Belliot, J. Le Pendu, *Rev. Med. Virol.* **23**, 355–366 (2013).
28. A. Reeck *et al.*, *J. Infect. Dis.* **202**, 1212–1218 (2010).
29. C. Richardson, R. F. Bargatze, R. Goodwin, P. M. Mendelman, *Expert Rev. Vaccines* **12**, 155–167 (2013).
30. R. L. Atmar *et al.*, *N. Engl. J. Med.* **365**, 2178–2187 (2011).
31. R. L. Atmar, M. K. Estes, *Gastroenterol. Clin. North Am.* **35**, 275–290 (2006).
32. M. Tan, X. Jiang, *Trends Microbiol.* **13**, 285–293 (2005).
33. P. H. Otto *et al.*, *J. Virol.* **85**, 12013–12021 (2011).
34. U. C. Karandikar *et al.*, *J. Gen. Virol.* 10.1099/jgv.0.000545 (2016).
35. S. Taube *et al.*, *MBio* **4**, e00450-13 (2013).
36. K. Bok *et al.*, *Proc. Natl. Acad. Sci. U.S.A.* **108**, 325–330 (2011).
37. K. Y. Green, *Clin. Infect. Dis.* **62**, 1139–1140 (2016).
38. J. R. Brown, K. Gilmour, J. Breuer, *Clin. Infect. Dis.* **62**, 1136–1138 (2016).
39. W. T. Flynn, L. J. Saif, *J. Clin. Microbiol.* **26**, 206–212 (1988).
40. K. O. Chang *et al.*, *Proc. Natl. Acad. Sci. U.S.A.* **101**, 8733–8738 (2004).

ACKNOWLEDGMENTS

Supported in part by Public Health Service grant PO1 AI 057788 (M.K.E.) and Agriculture and Food Research Initiative competitive grant 2011-68003-30395 from the USDA National Institute of Food and Agriculture. We acknowledge the assistance of the Study Design and Clinical Research Core and Cellular and Molecular Morphology Core of the Texas Medical Center Digestive Diseases Center and the Cytometry and Cell Sorting Core, which are supported in part by Public Health Service grants P30 DK-56338, P30 CA-125123 (to C. K. Osborne), National Institute of Allergy and Infectious Diseases grant AI036211, and the Dan L. Duncan Cancer Center at Baylor College of Medicine. We thank B. V. V. Prasad, T. Palzkill, S. Marriott, and M. Donowitz for critical reading of the manuscript. Author contributions: S.E.C., R.L.A., and M.K.E. supervised the project; K.E., K.M., J.R.B., U.K., V.R.T., L.Q., B.K., X.-L.Z., and F.H.N. designed and performed experiments and analyzed data; S.E.C., R.L.A., S.R., S.E.B., and M.K.E. designed experiments and analyzed data; A.R.O.,

D.B., and D.Y.G. provided reagents and conceptual advice; M.K.E., S.E.C., and K.E. wrote the initial draft of the manuscript; and all authors provided critical review and final approval of the manuscript. All relevant data are within this paper and the supplementary materials. Enteroids are available via a materials transfer agreement from Baylor College of Medicine. Baylor College of Medicine has filed a patent application related to this work: Cultivation of human noroviruses; provisional patent application no. 62/236,294.

SUPPLEMENTARY MATERIALS

www.sciencemag.org/content/353/6306/1387/suppl/DC1
Materials and Methods
Figs. S1 to S11
Table S1
References (*41*–*47*)

25 February 2016; accepted 18 August 2016
Published online 25 August 2016
10.1126/science.aaf5211

NEUROSCIENCE

The TRPM2 channel is a hypothalamic heat sensor that limits fever and can drive hypothermia

Kun Song,[1]*† Hong Wang,[1]† Gretel B. Kamm,[1]† Jörg Pohle,[1] Fernanda de Castro Reis,[2] Paul Heppenstall,[2,3] Hagen Wende,[1] Jan Siemens[1,3]‡

Body temperature homeostasis is critical for survival and requires precise regulation by the nervous system. The hypothalamus serves as the principal thermostat that detects and regulates internal temperature. We demonstrate that the ion channel TRPM2 [of the transient receptor potential (TRP) channel family] is a temperature sensor in a subpopulation of hypothalamic neurons. TRPM2 limits the fever response and may detect increased temperatures to prevent overheating. Furthermore, chemogenetic activation and inhibition of hypothalamic TRPM2-expressing neurons in vivo decreased and increased body temperature, respectively. Such manipulation may allow analysis of the beneficial effects of altered body temperature on diverse disease states. Identification of a functional role for TRP channels in monitoring internal body temperature should promote further analysis of molecular mechanisms governing thermoregulation and foster the genetic dissection of hypothalamic circuits involved with temperature homeostasis.

Core body temperature (T_{core}) is normally maintained very accurately in mammals within a narrow range around 37°C and serves as an important vital sign that is routinely monitored in hospitalized patients. Pathological conditions such as infections and systemic inflammation cause fever (*1*, *2*), an increase in the body's temperature that is thought to be mediated by prostaglandin E_2 (PGE_2)–induced inhibition of warm-sensitive neurons (WSNs) in the hypothalamic thermoregulatory center (*3*). Adverse drug-induced fluctuations in T_{core} can have severe and even fatal consequences (*4*). Conversely, clinically controlled modulation of T_{core} has beneficial effects and can prevent tissue damage, promote trauma recovery (*5*, *6*), or help decrease obesity (*7*).

The preoptic area (POA) of the hypothalamus serves as a thermostat, integrating temperature information to orchestrate the autonomous and behavioral adaptations needed to achieve thermal homeostasis (*3*, *8*). POA neurons receive and integrate information from peripheral temperature sensors located in the skin, spinal cord, and viscera. Local POA warming and cooling experiments (*9*–*13*) and genetic manipulations (*14*) have shown that this region of the central nervous system also detects local brain temperature changes, which have a strong impact on T_{core}. In fact, temperature changes in the POA can exert a dominant effect on T_{core} and can override lower-priority temperature inputs from peripheral temperature sensors, such as those located in the skin (*15*, *16*). Warming of the POA induces heat dissipation mechanisms such as cutaneous vasodilation, evaporative heat loss mechanisms, and behavioral adaptations, whereas cooling of the POA triggers heat conservation and thermogenesis.

POA neurons exhibiting pronounced temperature sensitivity have been described in in vivo models and in vitro preparations (*17*–*19*). WSNs enhance their firing rate upon warming, a process that is thought to relay temperature information to peripheral organs to promote heat loss (*3*). Conversely, a drop in deep brain temperature inhibits WSNs, a process that correlates with induction of thermogenesis and heat gain.

However, the genetic identity of WSNs and the molecular basis of their temperature sensitivity have remained elusive. Our work defined a population of WSNs that controls temperature homeostasis and identified a transient receptor potential (TRP) ion channel that subserves thermodetection in hypothalamic neurons.

TRPM2 is a heat sensor in a subset of POA neurons

To identify thermosensory molecules in the thermoregulatory center of the hypothalamus, we established calcium imaging as a means to monitor warming-induced responses of primary POA neuronal cultures (fig. S1, A to F). We applied a stringent criterion to identify WSNs by fura-2–mediated calcium imaging. We only counted neurons as WSNs if their relative increase in signal on receiving a thermal stimulus (up to 45°C) was larger than the mean fura-2 signal plus 5 times the standard deviation (5SD) of thermally unresponsive human embryonic kidney–293 cells subjected to the same temperature stimulus (fig. S1, E and F). This procedure allowed us to account and correct for the small unspecific temperature effect on the fluorescent fura-2 signal (*20*) (see fig. S1F and table S1 for details). We found that 16.3 ± 4.7% (mean ± SEM; n = 6 mice) of cultured POA neurons responded to warming, a fraction that is in the same range (10 to 16%) observed in electrophysiological studies of rodent POA cultures (*21*, *22*) and slightly lower than WSN percentages (20 to 40%) observed in POA slice preparations (*17*, *23*). Extracellular calcium appeared to be the source of the temperature-triggered increase in intracellular concentrations of free calcium, because chelation of external calcium abolished the response, whereas depletion of intracellular calcium stores did not have any effect on warm sensitivity (fig. S1, D and G).

Several ion channels are thermosensitive, exemplified by a steep temperature dependence (Q_{10} coefficient) of their opening probabilities. In particular, cationic TRP ion channels have been identified as thermosensors in the peripheral nervous system and function in the detection of ambient temperature changes (*24*–*27*).

To identify candidate channels mediating the observed warm sensitivity in neuronal POA cultures, we tested various inhibitors and agonists of TRPs and other thermosensitive ion channels (fig. S1, H to L). The calcium response appeared to be mediated by direct Ca^{2+} flux through a thermosensitive ion channel and not an indirect readout of voltage-gated channels, because nifedipine and tetrodotoxin, which are blockers of voltage-gated calcium and sodium channels, respectively, had only a small effect on the responses to increased temperature (fig. S1, H, J, K, and L). 2-aminoethoxydiphenyl borate (2-APB), a potent inhibitor of several ion channels and activator of TRPV-type channels (*28*–*30*), abolished the temperature response of POA neurons in a reversible manner (Fig. 1A).

[1]Department of Pharmacology, University of Heidelberg, Im Neuenheimer Feld 366, 69120 Heidelberg, Germany. [2]European Molecular Biology Laboratory (EMBL), Adriano Buzzati-Traverso Campus, Via Ramarini 32, 00016 Monterotondo, Italy. [3]Molecular Medicine Partnership Unit, EMBL, Meyerhofstraße 1, 69117 Heidelberg, Germany. *Present Address: Max Delbrück Center for Molecular Medicine, Robert Rössle Straße 10, 13125 Berlin, Germany. †These authors contributed equally to this work. **‡Corresponding author. Email: jan.siemens@pharma.uni-heidelberg.de**

Replication of human noroviruses in stem cell–derived human enteroids

Khalil Ettayebi, Sue E. Crawford, Kosuke Murakami, James R. Broughman, Umesh Karandikar, Victoria R. Tenge, Frederick H. Neill, Sarah E. Blutt, Xi-Lei Zeng, Lin Qu, Baijun Kou, Antone R. Opekun, Douglas Burrin, David Y. Graham, Sasirekha Ramani, Robert L. Atmar and Mary K. Estes

Science **353** (6306), 1387-1393.
DOI: 10.1126/science.aaf5211originally published online August 25, 2016